nature sustainability

Article

https://doi.org/10.1038/s41893-026-01867-y

Broad-spectrum insecticide detoxification for the protection of managed pollinators

Received: 4 July 2024

Accepted: 18 May 2026

Published online: 18 June 2026

Check for updates

Zuliang Huang[1,4], Yan Wang[1,4], Jiakun Guo[1], Suhui Lv[2], Jie Gui[2], Zhiyuan Zhong[1] ✉, Jing Chen[2,3] ✉ & Chao Deng[1] ✉

Sustainable agriculture relies heavily on various pollinators that support the production and diversity of approximately 75% of global food crops. However, pollinator populations are in sharp decline largely due to insecticide exposure during crop pollination and a lack of effective protective interventions. Here we report a biomimetic detoxification system—mesoporous silica microparticles (MTSMs) coated with locust cell membrane and tannic acid—to protect bumblebees against insecticides. By leveraging π–π stacking and specific enzyme interactions, MTSMs presented high removal efficiency across organophosphate, pyrethroid and neonicotinoid classes, while maintaining minimum non-specific clearance of favourable enzymes predominantly present in the gastrointestinal system of bees. In addition to revealing dose-dependent detoxification capacity towards organophosphate and neonicotinoid insecticides, MTSMs exhibited over 12-h residency in the gastrointestinal tract of bumblebees to facilitate insecticide scavenging, and could be mostly excreted by bees within 48 h, causing no death of bees even at a high concentration of 50 mg ml^{-1}. Environmental safety assessments indicate that MTSMs exhibit no observable inhibition effects on other insect viability (for example, *Teleogryllus mitratus* and *Teleogryllus emma*) and leguminous plant morphogenesis, suggesting their potential compatibility with agricultural applications. Overall, MTSMs have the potential to provide efficient broad-spectrum insecticide detoxification for the protection of managed pollinators.

Pollinators play a vital role in maintaining ecosystem resilience and supporting global agriculture production, contributing approximately US$351 billion annually to the latter[1–3]. However, the overuse of insecticides (600,000 t yr^{-1}, globally) for pest control creates unintended survival stresses for pollinators, reducing their range and abundance[4,5]. Addressing this crisis demands effective strategies to mitigate exposure to three leading insecticide categories: organophosphates (OPs), pyrethroids (PYs) and neonicotinoids (NNIs)[6–8].

Current mitigation efforts focus on eliminating insecticides from environmental matrices such as water, pollen, agricultural crops and wildflower nectar. Surface discharge cold plasma oxidation[9], magnetic nanoparticles[10] and acetylcholinesterase (AChE)-functionalized nanosponges[11,12] have been explored to degrade or adsorb insecticides. Although these methods reduce environmental contamination, they fail to address internal insecticide accumulation in pollinators. Recently, calcium carbonate microspheres encapsulated with

[1]Biomedical Polymers Laboratory, and Jiangsu Key Laboratory of Advanced Functional Polymer Materials, College of Chemistry, Chemical Engineering and Materials Science, and State Key Laboratory of Radiation Medicine and Protection, Soochow University, Suzhou, China. [2]National Key Laboratory of Technologies for Chinese Medicine Pharmaceutical Process Control and Intelligent Manufacture, Nanjing University of Chinese Medicine, Nanjing, China. [3]College of Pharmacy, Nanjing University of Chinese Medicine, Nanjing, China. [4]These authors contributed equally: Zuliang Huang, Yan Wang.
✉e-mail: zyzhong@suda.edu.cn; jingchen3236@njucm.edu.cn; cdeng@suda.edu.cn

https://doi.org/10.1038/s41893-026-01867-y

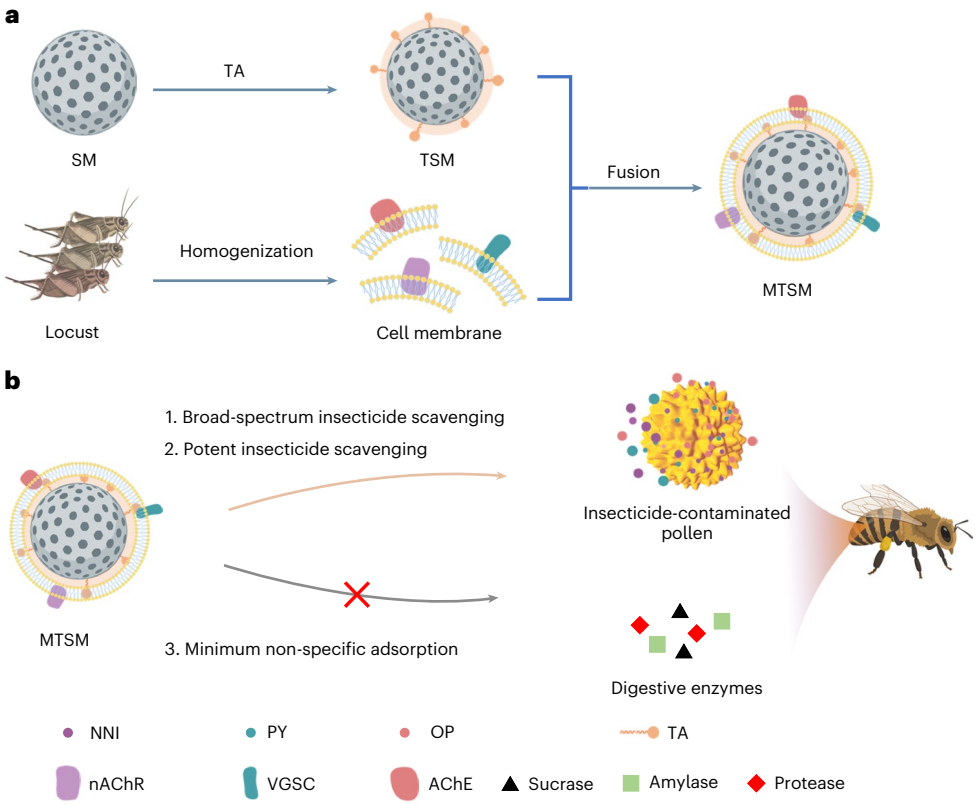

Fig. 1 | Schematic illustration of construction and insecticide scavenging of MTSMs. a, MTSM construction. **b**, Selective insecticide scavenging from pollinators by MTSMs. Schematics created in BioRender; **a**,**b**, Sun, Y. https://biorender.com/mq8mp7f (2026); **b**, Sun, Y. https://biorender.com/xu1nytv (2026).

phosphotriesterase have been developed to afford direct mitigation of OP insecticides in bees via enzymatic degradation[13]. However, the coexistence of multiclass insecticides in modern agriculture necessitates scavengers with broad-spectrum efficacy, high biocompatibility and scalable fabrication.

Mesoporous silica microparticles (SMs) offer high surface areas, accessible modification and excellent safety[14–16]. Tannic acid (TA), a natural polyphenol, provides multiple pyrogallols for robust surface functionalization and drug binding via covalent and π–π interactions[17–22]. Locust cell membrane exhibits unique insecticide affinity through selective degradation of OP by AChE[11,23,24], and specific binding of NNI and PY with nicotine receptors of acetylcholine (nAChRs) and voltage-gated sodium channels (VGSCs), respectively[21,25,26]. Notably, locust AChE possessing unique amino acid residues confers superior affinity for OPs compared with other species[27].

In this study, we engineer locust membrane-coated, TA-modified mesoporous silica microparticles (MTSMs) as versatile and potent insecticide scavengers to protect managed pollinators (Fig. 1). MTSMs persisted over 12-h residency in the gastrointestinal tract of bumblebees, enabling sustained detoxification. In bumblebees fed with insecticide-contaminated pollen, MTSMs boosted survival to 90% via dose-dependent toxin removal. This potent, versatile and broad-spectrum detoxification strategy addresses the urgent need to safeguard pollinators from cocktails of agricultural insecticides.

Results and discussion

Fabrication of MTSMs

TA-coated microparticles (TSMs) was fabricated through the covalent conjugation of TA with amino groups of mesoporous SMs via Schiff base and Michael addition chemistry[28]. Characteristic Fourier transform infrared (FTIR) spectroscopy signals of hydroxyl group at 3,500 cm^{-1}, carbonyl group at 1,720 cm^{-1} and phenyl group at 1,530–1,620 cm^{-1} (Fig. 2a) denoted the successful introduction of TA on SM. Moreover, TSMs with a range of of TA content (0.76–12.0 wt%) could be readily acquired by adjusting the feed ratios of TA to SM as characterized by thermogravimetric (Fig. 2b and Supplementary Fig. 1) and bicinchoninic acid (BCA, Fig. 2c) assays, in which the TA amount increased with increasing TA/SM weight ratio, and reached a plateau when the TA/SM weight ratio was greater than 0.2. The locust cell membrane, which features various binding sites for different insecticides, has been utilized to selectively recognize insecticides released from polluted pollen[29,30]. The coating of locust cell membrane on TSMs was facilely accomplished under mild ultrasound conditions to form MTSMs[31]. Confocal imaging revealed that notable red spots derived from the fluorescent probe DiD inserted in locust cell membrane clearly appeared on the microparticles (Fig. 2d,e), denoting the effective formation of cell membrane patches on the particulate surfaces. The membrane amount in MTSM can be adjusted by changing the concentrations of cell membrane, which correlated directly quantified with membrane proteins, and nearly attained the maximum (approximately 5% of the total mass of MTSMs) when the protein increased to 0.25 mg (Fig. 2f). The bioactivity of AChE on microparticles was determined through monitoring the degradation of acetylthiocholine into thiocholine by AChE as done in previous reports (Fig. 2g)[32–34], and the results revealed that the process of membrane coating induced negligible changes in the catalytic activity of AChE in cell membrane towards acetylthiocholine (Fig. 2h). Notably, MTSMs following 7 days of storage in sucrose solution exhibited sustained fluorescence intensity in DiD-labelled cell membrane domains and minimal enzymatic activity change of AChE within the cell membrane coated on microspheres (Supplementary Fig. 2a,b), denoting the good stability of cell membrane coating on MTSMs. Furthermore, no detached cell membrane fragments were detected in the microsphere supernatant after 7 days of incubation in sucrose solution (Supplementary Fig. 2c), providing additional evidence for the

https://doi.org/10.1038/s41893-026-01867-y

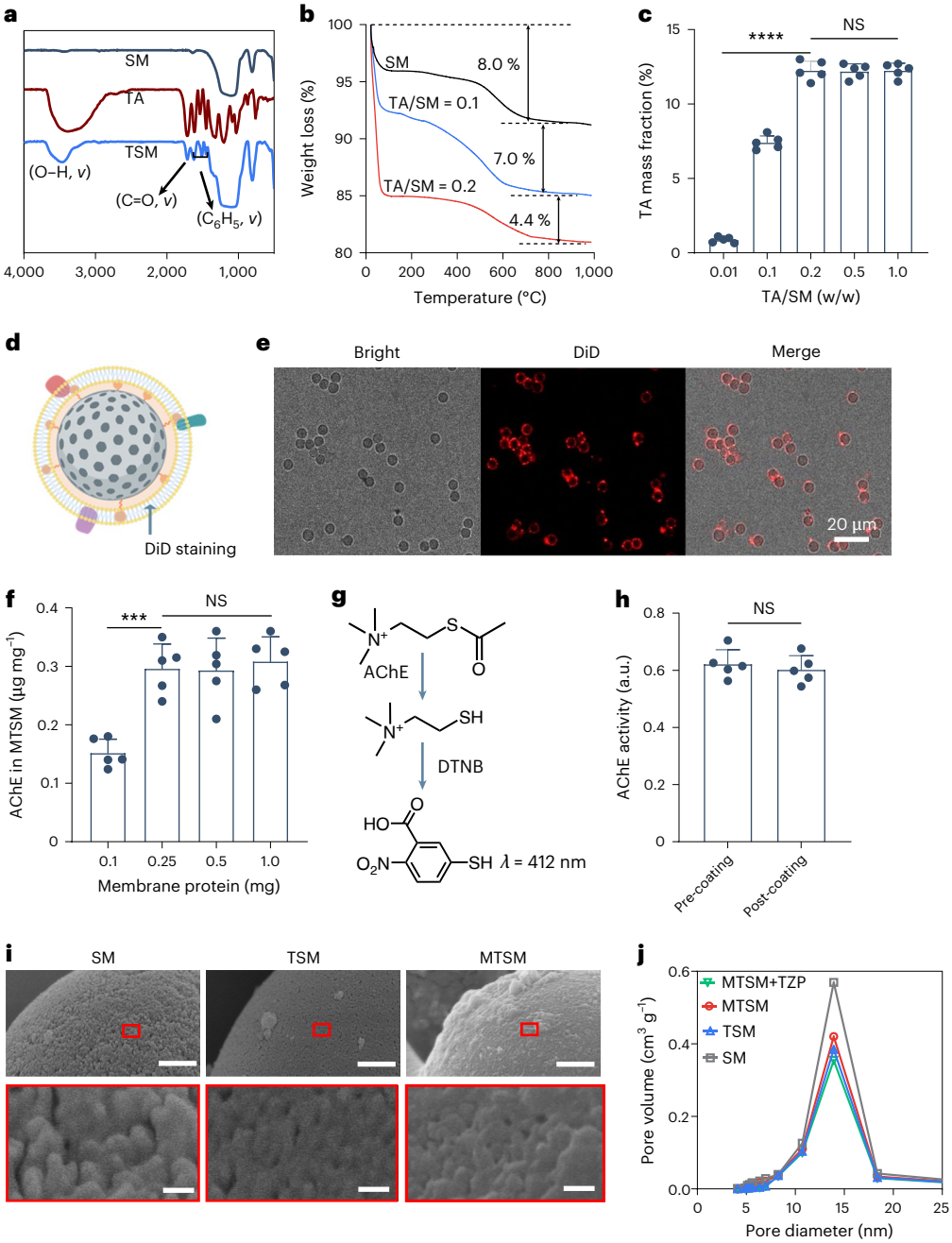

Fig. 2 | Characterization of MTSMs. a, FTIR spectra of mesoporous SMs, TA and TSMs. **b**, Thermogravimetric curves of TSMs prepared at TA/SM weight ratios of 0.1 and 0.2. **c**, TA mass fraction in TSM prepared at different TA/SM weight ratios determined by bicinchoninic acid assay. Data are presented as mean ± s.d. ($n = 5$). Differences in TA mass fraction between groups were determined using a one-way ANOVA. Statistical significance was defined as $^{***}P < 0.001$; NS, not significant. **d**, Structure diagram of MTSMs whose outmost layer (locust cell membrane) was stained with DiD fluorescence dye for tracking. **e**, Confocal microscopy images of MTSMs inserted with DiD (red). Scale bars, 20 μm. This experiment was conducted three times with almost the same results. **f**, AChE content in MTSMs prepared using different amounts of locust cell membrane quantified with protein concentrations. Data are presented as mean ± SD ($n = 5$). Differences in AChE content between groups were determined using a one-way ANOVA. Statistical significance was defined as $^{****}P < 0.0001$. **g**, Diagram of the method used to characterize AChE activity. In the presence of AChE, acetylthiocholine was degraded into thiocholine, which induced the cleavage of the disulfide bonds of DTNB to form TNB with UV absorbance at 412 nm. **h**, AChE bioactivity change following the membrane coating via ultrasound quantified by measuring the catalytic activity towards acetylcholine. Data are presented as mean ± s.d. ($n = 5$). Differences in AChE activity between groups were determined using an unpaired Student's t-test. Statistical significance was defined. **i**, Surface structure characterization of microparticles observed by scanning electron microscopy. The lower panel displays magnification of selected rectangular regions from the corresponding upper micrographs. Scale bars, 500 nm (upper), 50 nm (lower). This experiment was conducted three times with almost same results. **j**, Pore size distribution of microparticles determined by the Brunauer–Emmett–Teller method. Schematic in **d** created in BioRender; Sun, Y. https://BioRender.com/03jma7p (2026).

durability of the CM coating. Scanning electron microscopy images displayed that TA and cell membrane coating, although notably remodelling the surface morphology, had little influence on the mesoporous structures inside the microspheres (Fig. 2i and Supplementary Fig. 3). Consistently, N_2 adsorption isotherms revealed that both MTSM and TSM possessed slightly decreased pore volume and comparable pore sizes ranging from 5 to 20 nm (Fig. 2j and Supplementary Fig. 4), providing accessible space for drug adsorption as previous reports[35].

In vitro removal efficiency of insecticides by MTSMs

Over one-third of insecticides in use contain OP compounds which accumulate in high levels and are toxic to pollinators[36,37]. In this study, triazophos (TZP), methyl parathion (MPT) and chlorpyrifos (CP) were used as examples of typical OP insecticides to evaluate removal efficiency. Leveraging strong π–π stacking between OP insecticides and TA, and biomimetic recognition and binding of OP insecticides by AChE, MTSMs were expected to afford efficient insecticide scavenging (Fig. 3a). π–π stacking has been utilized to accomplish robust drug loading in various drug-delivery systems including micelles, polymersomes and nanoparticles[38–41]. Figure 3b demonstrates that increasing the TA/SM weight ratio enhances TZP removal, with efficiency plateauing at ratios higher than 0.2. Locust cell membrane decoration further improved absorption, with membrane protein concentrations of no lower than 0.25 mg ml^{-1} yielding over 83% removal (Fig. 3c). Thus, MTSMs with TA/SM = 0.2 and a membrane protein concentration of 0.25 mg ml^{-1} were utilized to evaluate effects of removal time, microparticle concentration and insecticide concentration. As expected, TZP adsorption increased with MTSM concentrations, although only a modest improvement (around 4%) was obtained when increasing the concentration from 20 to 40 mg ml^{-1} (Fig. 3d). MTSMs efficiently removed TZP at concentrations of 0.01–0.5 mg ml^{-1} (Fig. 3e), with over 57% clearance within 5 min and around 95% after 12 h (Fig. 3f). MSMs formed by coating SMs with cell membrane only were used to explore the effect of cell membrane on clearance efficiency. Regardless of incubation time, microparticle concentration and drug concentration, the removal efficiency followed the sequence MTSM > TSM ≫ MSM > SM. The removal mechanism of MTSMs related to TA and cell membrane was further explored. Mechanistic investigation revealed a remarkable redshift of TZP from 278 to 290 nm in ultraviolet–visible (UV–vis) spectra (Fig. 3g), indicating strong π–π stacking with TA. Isothermal titration calorimetry (ITC) confirmed spontaneous TA-TZP interaction (ΔG = −20 kJ mol^{-1}), accompanied by heat absorption (ΔH = 2,184 kJ mol^{-1}) and an increase in entropy (ΔS = 7,396 J mol^{-1} K^{-1}), consistent with intermolecular π–π stacking (Fig. 3h–i). AChE, which is known to recognize and degrade OP insecticides[11,12], mediated TZP degradation (Fig. 3j), as confirmed by high-performance liquid chromatography (HPLC) detection of obviously reduced TZP and increased phenyltriazolol over time (Fig. 3k). A maximum phenyltriazolol/TZP ratio of 2:7 was attained after 12 h incubation (Supplementary Fig. 5), highlighting the essential combination of physical sorption and biodegradation. MTSMs and TSMs also efficiently scavenged MPT and CP, with MTSMs achieving around 80% removal (Fig. 3l).

NNI and PY insecticides, more toxic towards pollinators than converntional OP insecticides (lower LD_{50})[7], were further evaluated. For imidacloprid (IMI, a typical NNI), TA introduction markedly elevated removal efficiency, plateauing at 43.1% when TA/SM weight ratios were higher than 0.2 (Fig. 4a). NNIs and PYs were reported to bind the nAChRs and VGSCs on the insect cell membrane, respectively, to kill insects[42]. MTSMs presented nearly 10.0 μg g^{-1} of nAChRs and 5.2 μg g^{-1} of VGSCs on the surface when the locust cell membrane protein concentration was 0.25 mg ml^{-1} (Fig. 4b), enabling over 55% IMI removal (Fig. 4c). Thereafter, MTSMs constructed as above were utilized to evaluate the effect of removal time, pH, microparticle concentration and insecticide concentration. As expected, the IMI adsorption was enhanced with increasing microparticle concentrations and reached 67.1% at 40 mg ml^{-1} (Fig. 4d). Furthermore, MTSMs could maintain high removal efficiency even at a high IMI concentration of 0.5 mg ml^{-1} (Fig. 4e); the removal efficiency increased over time and reached 77.3% at 48 h (Fig. 4f). Notably, decreasing the pH to 4.8 had little influence on the absorption efficiency (Fig. 4g), suggesting that the removal efficiency of insecticides by MTSMs would not be compromised in the stomach and gut of bees (pH 4.8–6.5). Similarly, MTSMs and TSMs exhibited efficient scavenging of other NNI insecticides (acetamiprid, thiamethoxam), with MTSMs affording around 45.2% removal of acetamiprid (Fig. 4h). Meanwhile, we assessed the scavenging capacity of PY by microparticles using CP as a typical example, and found that around 50% of CP was removed by MTSMs within 60 min (Fig. 4i and Supplementary Fig. 6), corroborating their broad-spectrum scavenging capacity. Although MTSMs are effective at sequestering the major insecticide classes, including OP, NNI and PY, future studies must explore interactions with other pesticides given their diversity and continuous development. To elucidate the sorption mechanisms of microspheres (MTSMs, TSMs, MSMs and SMs) toward structurally distinct insecticides (TZP, IMI, CFT), systematic investigations of adsorption interactions were performed using selective inhibitors including NaCl (electrostatic interactions), urea (hydrogen bonding), Tween-80 (hydrophobic interactions) and pyrene (π–π stacking) (Supplementary Fig. 7). Although SMs, MSMs, TSMs and MTSMs displayed a range of surface charges (Supplementary Fig. 8), NaCl-mediated shielding experiments revealed negligible electrostatic contributions to insecticide adsorption, probably due to near-neutral insecticide charges. Instead, MTSMs demonstrated a synergistic adsorption mechanism for insecticide removal, combining TA-mediated π–π/hydrophobic interactions evidenced by

Fig. 3 | Removal efficiency of OP insecticides by MTSMs. a, Scheme of biomimetic recognition of insecticides by MTSMs. **b**, Effect of TA coating on TZP removal. The ratio of TA/SM ranging from 0 to 1 indicates that the content of SM remains constant while the amount of TA in TSM is continuously increased. Data are presented as mean ± s.d. (n = 5). **c**, Effect of locust cell membrane coating on TZP removal. We used the concentration of membrane proteins to represent the content of the cell membrane, with the membrane protein concentration ranging from 0 to 1 mg ml^{-1}. Data are presented as mean ± s.d. (n = 5). **d**, Effect of microparticle concentrations on TZP removal. The experiments in each group followed the principle of a single variable, with the microsphere concentration ranging from 2 to 40 mg ml^{-1}. Data are presented as mean ± s.d. (n = 5). **e**, Effect of TZP concentration. The experiments in each group followed the principle of a single variable, with the TZP concentration ranging from 0.01 to 0.50 mg ml^{-1}. Data are presented as mean ± s.d. (n = 5). **f**, Effect of incubation time. The experiments in each group followed the principle of a single variable, with the incubation time ranging from 5 to 720 min. Data are presented as mean ± s.d. (n = 5). **g**, UV–vis spectra of the mixture of TA and TZP in PBS (pH 6.5). **h**,**i**, Isothermal titration calorimetry of TZP (0.1 mM) (**h**) and TA (0.5 mM) (**i**). **j**, Degradation reaction of TZP triggered by AChE. TZP and its degradation product (phenyltriazolol) were monitored by HPLC with different elution times as illustrated. **k**, TZP and phenyltriazolol were monitored by HPLC following the coincubation of TZP with MTSMs for (a) 5 min, (b) 15 min, (c) 60 min and (d) 240 min, respectively. **l**. Removal efficiency of OP insecticides triazophos TZP, MPT and CP by MTSMs. Data are presented as mean ± s.d. (n = 5). IFor these experiments, the treatment time was 60 min, the pH was 6.5, and the concentrations of microparticles and insecticides were 20 mg ml^{-1} and 50 μg ml^{-1}, respectively, unless otherwise mentioned. The n = 5 experimental replicates for each group were exposed to identical environmental and experimental conditions. Specifically, there were five individual sample tubes for each group. After meeting the set conditions, an aliquot of each sample tube was taken for HPLC analysis. Differences in removal efficiency between groups were determined by ANOVA. Statistical significance was defined as $^{*}P < 0.05$, $^{**}P < 0.01$, $^{***}P < 0.001$, $^{****}P < 0.0001$. Schematic in **a** created in BioRender; Sun, Y. https://BioRender.com/6lmhnn0 (2026).

https://doi.org/10.1038/s41893-026-01867-y

Tween-80/pyrene inhibition with cell-membrane-driven biodegradation confirmed by enzyme inactivation effects.

Inhibition of non-specific adsorption

Ideal insecticide scavengers should not only possess potent removal capacity, but also need to exhibit minimal adsorption of favourable substances in the gastrointestinal system of pollinators (Fig. 5a). Sucrase, protease and amylase are crucial digestive enzymes generally present in the gastrointestinal system of bees[43]. As shown in Fig. 5b–d, obvious adsorption of sucrase, protease and amylase was observed with TSMs due to the interactions of enzymes with TA on the surface of the microparticles. In sharp contrast, MTSMs displayed significantly decreased absorption of all enzymes at concentrations varying from 1.0 to 100 μg ml^{-1}, indicating that the introduction of cell membranes

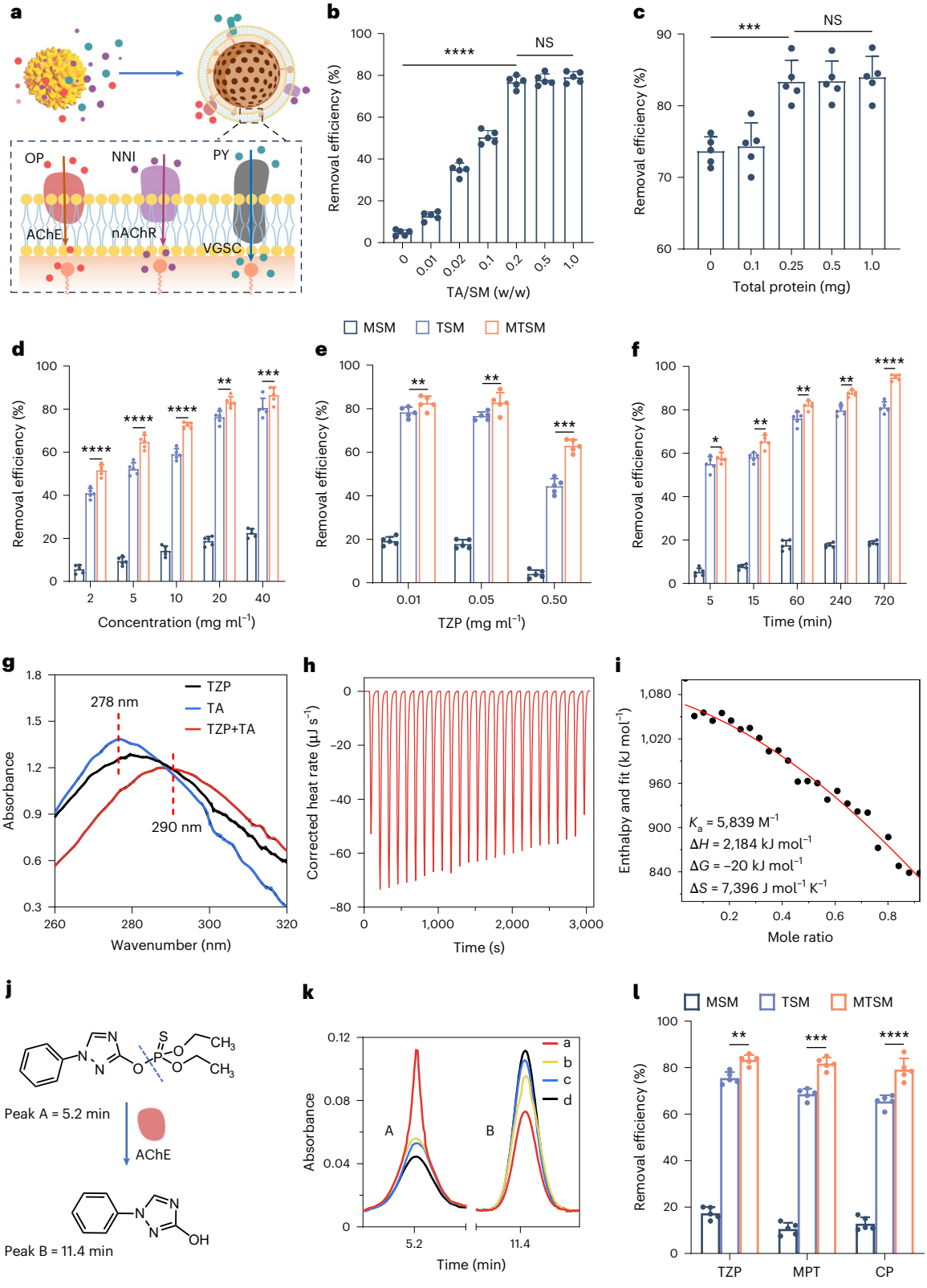

https://doi.org/10.1038/s41893-026-01867-y

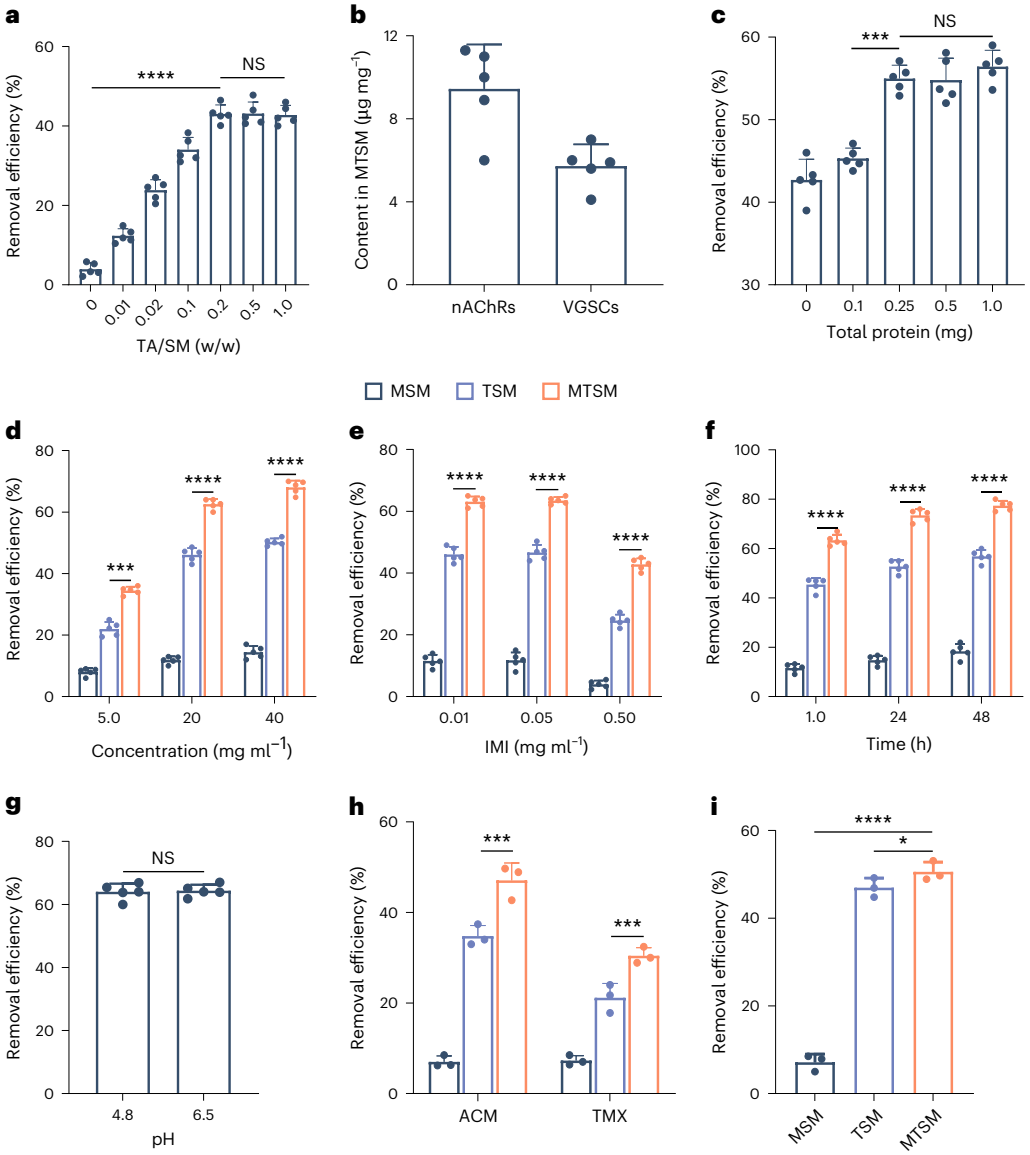

Fig. 4 | Removal efficiency of neonicotinoid insecticides by MTSMs. a, Effect of TA coating on IMI removal. The TA/SM ratios ranging from 0 to 1 indicated that the SM content maintained at a constant level, while the TA amount in TSMs was progressively increased. Data are presented as mean ± s.d. ($n = 5$). **b**, nAChR and VGSC content in MTSMs prepared at locust cell membranes containing 0.25 mg protein. **c**, Effect of locust cell membrane coating on IMI removal. The amount of cell membrane was represented by membrane proteins ranging from 0 to 1.0 mg. Data are presented as mean ± s.d. ($n = 5$). **d**, Effect of microparticle concentrations on IMI removal. The experiments in each group followed the principle of a single variable, with the microsphere concentration ranging from 5.0 to 40 mg ml^{-1}. Data are presented as mean ± s.d. ($n = 5$). **e**, Effect of IMI concentration. The experiments in each group followed the principle of a single variable, with the IMI concentration ranging from 0.01 to 0.50 mg ml^{-1}. Data are presented as mean ± s.d. ($n = 5$). **f**, Effect of treatment time on IMI removal. The experiments in each group followed the principle of a single variable, with the treatment time ranging from 1.0 to 48 h. Data are presented as mean ± s.d. ($n = 5$). The $n = 5$ experimental replicates for each group were exposed to identical environmental and experimental conditions. There were five individual sample tubes for each group. **g**, pH effect on IMI removal efficiency of MTSMs. **h**, Removal efficiency of acetamiprid (ACM) and thiamethoxam (TMX). Data are presented as mean ± s.d. ($n = 3$). **i**, Removal efficiency of CP. Data are presented as mean ± s.d. ($n = 3$). The $n = 3$ experimental replicates for each group were exposed to identical environmental and experimental conditions. If not otherwise mentioned, In these experiments, the treatment time was 60 min, the pH was 6.5, and the concentrations of microparticles and insecticides were 20 mg ml^{-1} and 50 μg ml^{-1}, respectively, unless otherwise noted. Differences in removal efficiency between groups were determined by ANOVA. Statistical significance was defined as $^{*}P < 0.05$, $^{**}P < 0.01$, $^{***}P < 0.001$, $^{****}P < 0.0001$.

greatly inhibited the non-specific clearance of favourable enzymes. A mixture of TZP and enzymes was prepared to mimic the gastrointestinal environment of bees to explore insecticide removal using microparticles. In comparison with TSMs, MTSMs presented obviously enhanced TZP removal while significantly decreasing the adsorption of sucrase (15% versus 27%), amylase (17% versus 48%) and protease (14% versus 42%) (Fig. 5e). The potent insecticide clearance and minimum adsorption of favourable enzymes (<20%) support the outstanding efficiency and safety of MTSMs. The selective adsorption is predominantly governed by the compact interfacial membrane coating on MTSMs, which inhibits the non-specific adsorption of macromolecular proteins such as digestive enzymes by blocking their access to the microsphere surface, while maintaining permeability for small-molecule pesticides.

In vivo gastrointestinal distribution

MTSMs were labelled with fluorescein isothiocyanate (FITC-MTSMs) through the reaction of FITC with the amino group of SMs to track the

https://doi.org/10.1038/s41893-026-01867-y

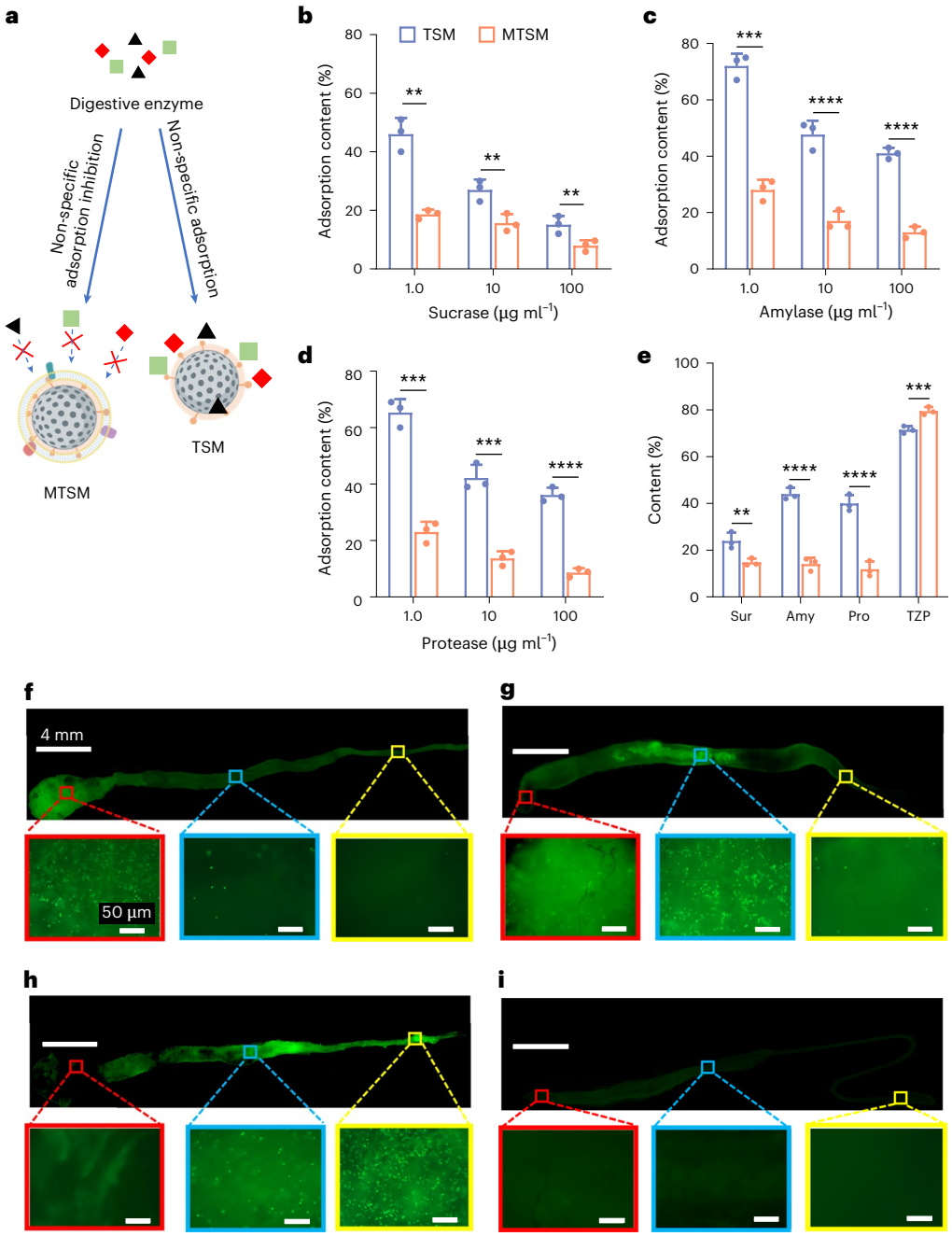

Fig. 5 | Inhibition of non-specific adsorption and in vivo gastrointestinal distribution of MTSMs. a, Schematic illustration of non-specific adsorption of different digestive enzymes. **b**–**d**, Inhibition of non-specific adsorption of digestive enzymes in the gastrointestinal system of pollinators: sucrase (**b**), amylase (**c**) and protease (**d**). The experimental conditions for different enzyme types are the same and independent of each other without any interference. The MTSM solution (20 mg ml^{-1}) was mixed with different enzymes (1–100 μg ml^{-1}) for 1 h at 37 °C. Data are presented as mean ± s.d. (n = 3). **e**, Selective removal of TZP under an environment of gastrointestinal enzymes. TZP (50 μg ml^{-1}) was mixed with digestive enzymes (sucrase, amylase and protease) at a concentration of 10 μg ml^{-1}. These measurements are independent of each other without any interference. Data are presented as mean ± s.d. (n = 3). The n = 3 experimental replicates for each group were exposed to identical environmental and experimental conditions. There were three individual sample tubes for each group. Differences in adsorption content between groups were determined using an unpaired Student's t-test. Statistical significance was defined as $^{**}P < 0.01$, $^{***}P < 0.001$, $^{****}P < 0.0001$. **f**–**i**, In vivo gastrointestinal distribution of MTSMs. FITC-labelled MTSMs in the gastrointestinal tract of bumblebees weretracked using fluorescent imaging within 0 h (**f**), 4 h (**g**), 12 h (**h**) and 48 h (**i**). Red rectangle: crop stomach or proventriculus; blue rectangle: midgut; yellow rectangle: hindgut. Scale bars, 4 mm (top), 50 μm (bottom). This experiment was conducted three times with almost same results. Schematic in **a** created in BioRender; Sun, Y. https://BioRender.com/lqrfhql (2026).

distribution and metabolism in the gastrointestinal tract of pollinators. After feeding bumblebees with FITC-MTSMs for 30 min, MTSMs were observed to pass sequentially through the crop stomach, proventriculus, midgut and hindgut of the gastrointestinal tract with time. During the initial period of digestion, most microparticles were distributed in the crop stomach, and negligible dissemination of microparticles was observed in the midgut and hindgut (Fig. 5f). Then, the majority of FITC-MTSMs moved out of the crop stomach and reached the midgut after 4 h. Notably, an apparent number of microparticles existed in the midgut and hindgut of the gastrointestinal tract from 4 to 12 h

https://doi.org/10.1038/s41893-026-01867-y

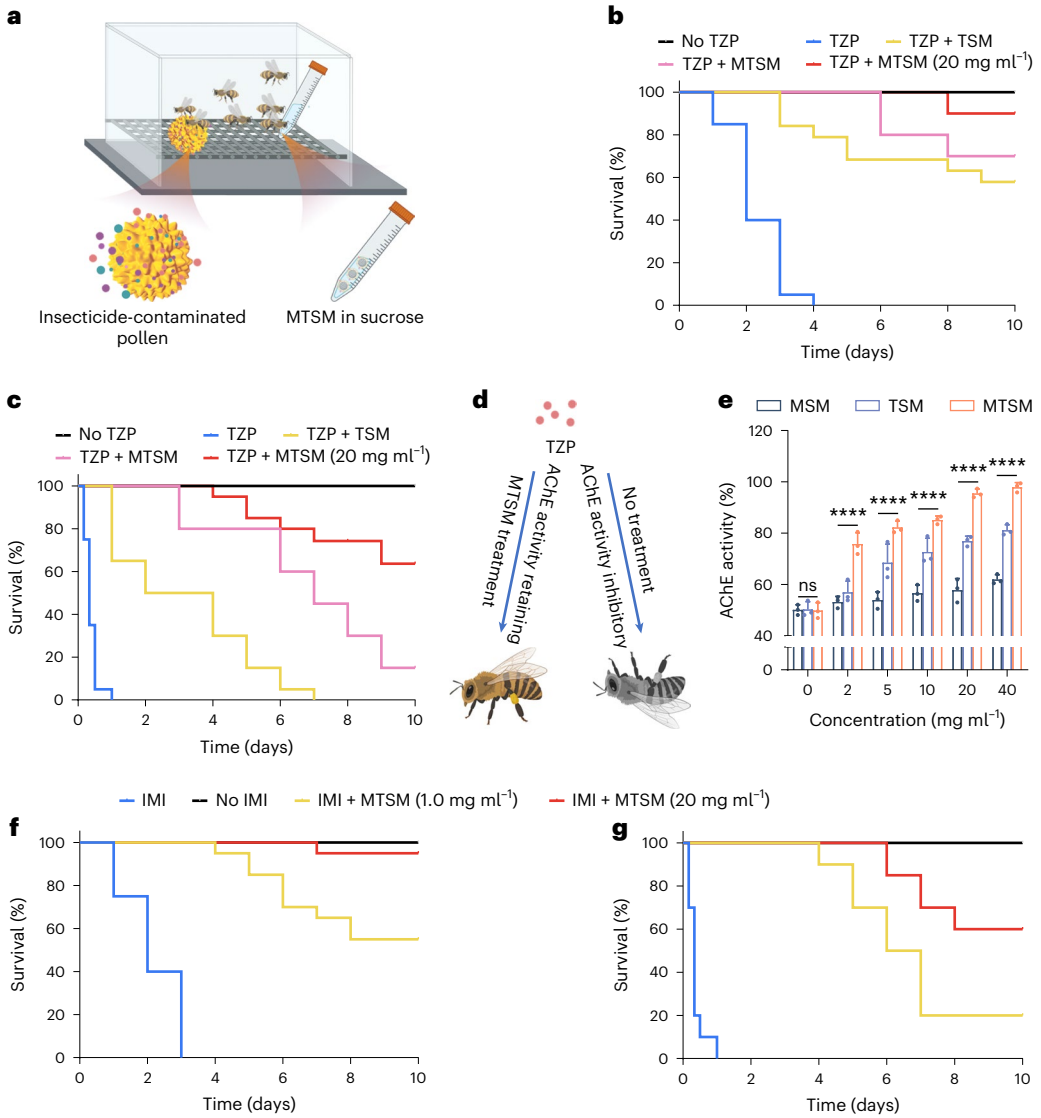

Fig. 6 | In vivo detoxification of insecticides in bumblebees using MTSMs. **a**, Schematic illustration of in vivo detoxification. **b**, Survival rate of bumblebees treated with TZP (60 μgTZP g^{-1} in pollen) and microparticles. **c**, Survival rate of bumblebees treated with TZP (120 μgTZP g^{-1} in pollen) and microparticles. **d**, Schematic illustration of AChE activity protection in bumblebees by MTSMs. **e**, AChE activity of bumblebee cell membrane following treatment with a supernatant of a mixture of TZP (20 mg ml^{-1}) microparticles at different concentrations. Data are presented as mean ± s.d. ($n = 3$). The $n = 3$ experimental replicates for each group were exposed to identical environmental and experimental conditions. Differences in AChE activity between groups were determined by ANOVA. Statistical significance was defined as $^{****}P < 0.0001$. **f**, Survival rate of bumblebees treated with IMI (5 μgIMI g^{-1} in pollen). **g**, Survival rate of bumblebees treated with IMI (15 μgIMI g^{-1} in pollen). Data in **b**,**c**,**f**,**g**,**e** are presented as mean ± s.d. ($n = 20$ individuals). Schematics created in BioRender: **a**, Sun, Y. https://BioRender.com/kgxdzls (2026); **d**, Sun, Y. https://BioRender.com/xu1nytv (2026).

(Fig. 5g–h). Pollen grains were reported to be similarly digested in the ventriculus for around 12 h (refs. 44,45), thus facilitating the absorption of insecticides in pollen by MTSMs in the gastrointestinal tract of bees. Therefore, administering detoxification particles to the bees once a day in the morning might be appropriate in practical applications. Specifically, these microparticles can be thoroughly blended into the nutrient sucrose fed to colonies prior to their daily pollination activities, ensuring efficient delivery alongside routine feeding protocols. After 48 h, no fluorescent microparticles was observed in the crop stomach, proventriculus, midgut and hindgut of the gastrointestinal tract, confirming that all microparticles were excreted from bees within 48 h (Fig. 5i).

In vivo detoxification efficacy

Bumblebees were used to assess in vivo detoxification efficacy because they process insecticides in similar fashion to honeybees[46,47]. Oral administration of MTSMs at concentrations of 0.1–50 mg ml^{-1} in sucrose solution (2.0 g ml^{-1}) elicited no mortality over 10 days, with minimal midgut cell death (indicated by red dots) and reactive oxygen species (ROS) fluctuations compared with the non-treated group (Supplementary Figs. 9–11). The expression of genes associated with social behaviours (*period*), mating (*mvl*, *period*) and foraging ability (*ame-let-7*, *Lkr*, *mvl*) of bumblebees[48,49] revealed negligible perturbations under MTSM exposure as verified by quantitative polymerase chain reaction analysis (Supplementary Fig. 12), indicating the reasonable in vivo safety of MTSMs. Moreover, MTSMs exhibited little influence on the foraging capability of bumblebees (Supplementary Fig. 13). Future safety studies should address long-term exposure effects across the developmental stages of pollinators (larval, pupal and adult phases).

In vivo detoxification efficacy was evaluated in bumblebees fed insecticide-contaminated pollen balls (Fig. 6a). Initially, pollen balls containing different concentrations of TZP (3, 15, 60, 120 μg g^{-1}) were

used to determine the levels of insecticide toxicity, and the results revealed that pollen balls containing 60 and 120 μgTZP g^{-1} caused 100% mortality at day 4 and 1, respectively (Supplementary Fig. 14). In addition, toxicological studies revealed that the median lethal doses (LD_{50}) of TZP for bumblebees was 0.620 μg per bee over 48 h (ref. 42). Based on the average daily pollen consumption of 10.2 mg per bee reported for bumblebees[50], dietary exposure of 60–120 μgTZP g^{-1} pollen within 48 h represents 2–4 times the LD_{50} values. In accordance with previous studies[42], pollen containing 60 and 120 μgTZP g^{-1} was therefore used to assess moderate and acute toxicity, respectively. At the moderate level of toxicity (60 μgTZP g^{-1} in pollen), TSM and MTSM treatment largely decreased the incidence of mortality and presented 60% and 70% survival rate within 10 days at a low concentration of 1.0 mg ml^{-1} in sucrose, respectively (Fig. 6b). As expected, increasing the concentration of microparticles to 20 mg ml^{-1} generated a better detoxification effect with a survival rate of up to 90%. For the acute toxicity condition (120 μgTZP g^{-1} in pollen), both TSMs and MTSMs induced extended survival times: bumblebees in the TSM group all died after 7 days whereas those in the MTSM group presented a 15% survival rate even 10 days later (Fig. 6c and Supplementary Fig. 15). The survival rate was further increased to 60% when a higher microparticle concentration of 20 mg ml^{-1} was used.

OP was reported to induce a massive accumulation of ACh and neurotoxicity by inhibiting carboxyl ester hydrolases such as AChE in different insects including pollinators[51,52]. To explore the protection capacity of MTSMs towards AChE bioactivity in bees, homogenized bumblebee cell fragments were incubated with supernatants of mixed TZP and microparticles (Fig. 6d). With increasing concentrations of microparticles, higher retention of AChE activity was obtained (Fig. 6e). For MTSMs, the retention activity of AChE reached over 80% when the microparticle concentration was higher than 5 mg ml^{-1}, and nearly complete activity retention (~99%) was acquired at a MTSM concentration of 40 mg ml^{-1}, indicating a dose-dependent protection of AChE by MTSMs. Moreover, the AChE activity in the heads of bumblebees that had been successfully detoxified by MTSMs showed no obvious difference compared to those of healthy bumblebees (Supplementary Fig. 16).

In addition to OP insecticides, NNI insecticides such as IMI were used to explore the in vivo detoxification capacity of microparticles. Notably, pollen balls containing 15 μgIMI g^{-1} and 5 μgIMI g^{-1} induced complete death of bumblebees within 1 and 3 days, respectively (Fig. 6f–g), revealing that IMI presented relatively higher toxicity than TPZ. Consistently, IMI was reported to have an LD_{50} of 0.223 μg per bee for bumblebees over 48 h (ref. 42), and pollen balls containing 5 and 15 μgIMI g^{-1} were similarly selected for the assessment of moderate and acute toxicity, respectively. MTSMs demonstrated apparent detoxification efficacy towards moderate and acute toxicity in bumblebees. For bumblebees fed with pollen balls containing 5 μgIMI g^{-1}, MTSMs at a concentration of 20 mg ml^{-1} in sucrose afforded a high survival rate of 95%. Thus, MTSMs afforded potent in vivo scavenging capacity of broad-spectrum insecticides in pollinators.

Environmental safety

MTSM was engineered through the integration of mesoporous silica particles, TA and locust cell membrane, all of which demonstrate acceptable biocompatibility and safety profiles. Mesoporous silica, recognized for its excellent biosafety, has been extensively utilized as a food additive and in biomedical fields[53]. TA, a naturally occurring polyphenolic compound, exhibits favourable biodegradability through both mammalian metabolic processes and microbial degradation, leading to minimal toxicological concerns[54]. Locust-derived components present negligible biosafety risks considering their long-standing history as edible insect species in various cultures and ecosystems[55]. Upon environmental exposure, silica particles undergo degradation into non-toxic monosilic and polysilic acids, TA decomposes into carbon dioxide and water, and locust cell membranes convert into small-molecule fatty acids, glycerol and phosphoric acid[54,56,57], potentially maintaining minimal influence on the environment and biodiversity. Based on the established safety profiles of individual components and their natural origins, we assume that MTSMs generate insignificant environmental or biosafety hazards. Furthermore, we assessed the influence of particles on the environment by monitoring the survival rates of two other insect models (*Teleogryllus mitratus* and *Teleogryllus emma*) and the phytotoxic effects on leguminous crops (soybean, *Glycine max* and mung bean, *Vigna radiata*). The MTSM-treated insects revealed 100% survival rates (n = 20 per group) after 10 days of exposure (Supplementary Fig. 17). Concurrent phytological analysis demonstrated complete germination equivalence between experimental and control groups (n = 20 per group) (Supplementary Fig. 18). Quantitative measurements showed no significant difference in the root and shoot growth lengths of soybeans and mung beans between the two groups (Supplementary Fig. 19).

The ecological impact of excreted MTSMs was further assessed on both insects and non-insect species. Notably, post-digestion MTSM residues exhibited no measurable adverse effects on the survival of insects such as *T. mitratus* and *T. emma* (Supplementary Fig. 20). Meanwhile, the supernatant of excreted MTSM-containing suspension showed no significant inhibition on the germination rates and growth lengths of mung beans and soybeans (Supplementary Figs. 21 and 22). These findings collectively indicate that MTSM exhibits no observable inhibition effects on insect viability (*T. mitratus* and *T. emma*) and leguminous plant (soybean, *G. max* and mung bean, *V. radiata*) morphogenesis, suggesting its potential compatibility with agricultural applications.

We have demonstrated that versatile and potent insecticide scavengers (MTSMs) constructed through facile surface decoration of mesoporous silica microparticles with TA and locust cell membrane sequentially afford effective protection for pollinators from a broad spectrum of insecticides including OPs, PYs and NNIs. By leveraging the π–π stacking with TA and specific binding by the acetylcholinesterases, nicotine receptors of acetylcholine, or voltage-gated sodium channels on locust cell membrane, MTSMs induced markedly improved removal of various insecticides combined with minimum non-specific clearance of favourable enzymes from the gastrointestinal system of pollinators. MTSMs was almost entirely excreted from bees within 48 h, and caused no death of bees even at a high concentration of 50 mg ml^{-1}, meaning the excellent safety of this material. Over a 12-h residency in the gastrointestinal tract of bumblebees, MTSMs exhibited extensive insecticide scavenging, affording dose-dependent detoxicification efficacy towards multiple insecticides and notably elevated survival rates of up to 90%. Although additional research such as the safety of the particles for ecosystems, field-wide assessments of bee colony survival, pollination efficiency, crop yield and quality, and economic viability after treatment remains warranted, the versatility and potency of MTSMs in insecticide detoxification for pollinators show great potential in practical applications. Because the raw materials are commercially accessible and affordable, the coating procedure is straightforward and scalable, and the costs are notably lower than conventional hive replacement, MTSMs offer a practical solution for large-scale agriculture.

Methods

MTSM preparation

MTSMs were prepared through sequential surface decoration of mesoporous SMs with TA and locust cell membrane. First, TA-decorated SMs (TSMs) were obtained by the covalent conjugation of TA with the amino group of SMs. Briefly, a TA solution in HEPES was added into 100 mg of SMs dispersed in HEPES buffer (20 ml, 5 mM, pH 7.4). The TA/SM weight ratios were fixed at 0.01, 0.1, 0.2, 0.5 and 1. After stirring at room temperature for 12 h, the reaction solution was centrifuged at 400 *g* for 6 min and washed three times with phosphate-buffered saline (PBS, 10 mM, pH 7.4). Then, the obtained dispersion was reacted with

a twofold excess of $NaBH_4$ at room temperature for 4 h. After sequential centrifuging, washing with PBS and drying at 35 °C in a vacuum oven, TSM product was obtained. Yield, 95.6%; FTIR, ν = 3,350 cm^{-1} (−OH), ν = 1,720 cm^{-1} (C=O), ν = 1,530 and 1,619 cm^{-1} (C−C, C=C of benzyl group).

A differential centrifugation method was utilized to extract the locust cell membrane[58–60]. Briefly, living locusts were frozen in liquid nitrogen, sterilized in 75% ethanol, ground and filtered with a cell strainer (70 μm) to obtain a cell suspension. To 20×10^6 extracted locust cells, 1.0 ml of membrane protein extraction solution was added according to a membrane and cytosol protein extraction kit (Beyotime, #P0033). Phenylmethylsulfonyl fluoride (PMSF) as a protease inhibitor was introduced within a few minutes at a final concentration of 1.0 mM to maintain the activity of the proteins on the cell membrane. After shaking for 30 min in an ice-water bath, the mixture was frozen and thawed three to disrupt the cells. Then, the membrane fragments were separated using differential centrifugation and stored at −80 °C until use. The total protein content of the membrane fragments was quantified using a Pierce BCA protein assay kit. The locust cell membrane was coated on the TSMs by an ultrasound machine (FB15063, Fisherbrand) with a power of 100 W in an ice-water bath for 15 min. The concentrations of membrane proteins varied from 0 to 1.0 mg ml^{-1}. To observe the membrane coating, DiD-stained MTSMs (DiD-MTSMs) were prepared by adding 0.5 wt% DiD (excitation/emission = 644/665 nm) to the locust cell membrane solution, which was then coated on microparticles by gentle sonication.

Measurement of AChE activity

AChE activity assay was performed in accordance with a previously described protocol[32,33]. In short, a working solution of 100 mM Tris–HCl, 20 mM KCl, 2.0 mM 5,5′-dithiobis-(2-nitrobenzoic acid) and 2.0 mM acetylthiocholine was prepared. Then, 100 μl of working solution was mixed with an equivalent volume of cell membrane solution containing AChE in a 96-well plate. The UV absorbance of the reduced phenyltriazolol product at 412 nm was recorded using a Varioskan Lux multimode reader every 1 min for 20 min to determine the change in AChE activity.

Insecticide removal

Different OP insecticides, including TZP, MPT and CP were used to evaluate the scavenging capacity of MTSMs. First, simulated intestinal fluid (SIF, pH 6.5) was prepared by dissolving KH_2PO_4 (6.8 g, 50 mM) and NaOH (0.9 g, 22.5 mM) in distilled H_2O (1.0 litre). Then, MTSMs were mixed with OP insecticides in SIF by gentle vortexing at 37 °C. After centrifuging at 400*g* for 6 min, the remaining insecticides in supernatant were quantified by HPLC (ProStar LC240, Waters Alliance). The removal efficiency of the OP insecticides was calculated with the formula: removal efficiency (%) = (1 − OP insecticides in supernatant/feed OP insecticides) × 100%. The effect of OP insecticide concentration (0.01–0.5 mg ml^{-1}), microsphere concentration (2.0–40 mg ml^{-1}) and mixing time (5.0–720 min) on removal efficiency was investigated in detail. All experiments were performed in triplicate. The removal capacity of MTSMs towards neonicotinoids and pyrethroids was similarly investigated except that HPLC with a detection wavelength of 270 nm was utilized for quantification.

The π–π interactions between OP insecticides and microspheres were investigated by monitoring the bathochromic shift of absorption peak generated by mixing TZP (20 μg ml^{-1}) and TA (20 μg ml^{-1}) solutions. The interaction forces between TA and TZP molecules was determined by ITC (TA Instruments). The binding and neutralization of OP insecticides with AChE on microspheres was monitored by measuring the leaving group phenyltriazolol. After mixing the microparticles (20 mg ml^{-1}) with TZP (50 μg ml^{-1}) for 5, 15, 60 or 120 min, the supernatant was collected and the amount of TZP and phenyltriazolol was quantified with HPLC.

In vitro detoxification effect

The in vitro detoxification effect was assessed by measuring the activity retention of AChE on bumblebee cell membrane, following the treatment with the supernatant of the mixture of TZP and MTSM solution. Typically, TZP (50 μg ml^{-1}) was mixed with MTSMs (2, 5, 10, 20, 40 mg ml^{-1}) at room temperature for 1 h. After centrifuging at 12,000*g* for 30 min, 200 μl of supernatant was mixed with an equivalent volume of the bumblebee cell membrane solution. The AChE activity was determined as described above.

Inhibition of non-specific adsorption

Sucrase, protease and amylase existing in the gastrointestinal tract of bumblebees were utilized to evaluate the inhibition of non-specific adsorption by MTSMs. The MTSM solution (20 mg ml^{-1}) was mixed with different enzymes (1–100 μg ml^{-1}) for 1 h at 37 °C. After centrifuging at 400*g* for 6 min, the activity of enzymes in supernatant was determined by the corresponding enzyme kit.

Animal experimental models

The animal experiments utilized commercial *Bombus terrestris* colonies (80 individuals per colony) from Biobest. The bumblebees were housed at 22–26 °C with 50 ± 5% relative humidity and 12 h light/dark cycles. Groups of 20 individuals were housed in nest boxes (50 cm × 35 cm × 25 cm) connected to flight boxes (60 cm × 43 cm × 30 cm) for free movement and foraging. Daily nutrition included pollen (5 g) and sucrose solution (2.0 g ml^{-1}) through dedicated feeding ports in specially designed hives with 2-mm ventilation grilles[50]. To maintain circadian rhythm consistency, experimental management occurred between 8.00 and 20.00. All equipment underwent pre-experiment cleaning with detergent and 75% alcohol. Healthy and active bumblebees from normal colonies were randomly selected as experimental subjects[13].

In vivo distribution and safety

FITC-labelled MTSMs (FITC-MTSMs) were prepared by the reaction of FITC with the amino group on the surface of microparticles, followed by coating with locust cell membrane. Twenty bumblebees were placed in separate test tubes. After starving for 3 h, the bees were fed with a sucrose solution (2.0 g ml^{-1}) containing 1.0 mg ml^{-1} FITC-MTSMs for 30 min. Then, the bumblebees were beheaded using dissection scissors at 0, 4, 12, 48 h. Gastrointestinal tracts were collected and placed on a glass slide for fluorescence imaging (490 nm) using a microscope (Eclipse, Nikon, Japan).

MTSM sucrose solutions were prepared across a concentration gradient ranging from 0.1 to 50 mg ml^{-1}. Bumblebees (n = 20 per group) were randomly allocated into breeding cages and fed with MTSM sucrose suspension at 12-h intervals. The in vivo safety of MTSMs was evaluated by observing the survival of the bumblebees over a 10-day period. Bumblebees were randomly assigned to species-appropriate rearing cages, and were provided with MTSM-supplemented sucrose solution (MTSM concentration, 20 mg ml^{-1}) every 12 h for 10 days. Then, the digestive tracts were dissected and processed for viability assessment using live/dead fluorescence cell staining. Meantime, midgut tissues were dissected and incubated with 10 μM dichlorodihydrofluorescein diacetate (DCFH-DA) at 37 °C for 30 min to measure the ROS production. In addition, the bumblebee heads were homogenized in phosphate solution, filtered and centrifuged at 12,000*g* for 30 min. The resultant cell suspensions were then subjected to qPCR analysis. The relevant genetic sequences can be found in the linked file.

To explore the foraging, the selected worker bees were housed in flight boxes (60 cm × 43 cm × 30 cm, 5 individuals per cage) and provided with ad libitum access to sucrose solution or MTSM-supplemented sucrose solution (MTSM concentration, 20 mg ml^{-1}). Fresh solutions were replenished every 12 h to ensure continuous food availability throughout the experimental period. The consumption

of sucrose solution was quantified following each feeding for 5 days, and the pollen intake was weighed and recorded at the end of the experiment.

In vivo detoxification efficacy

Microparticles (20 mg ml^{-1}) with an average diameter of ~8 μm dispersed in a 2 g ml^{-1} sucrose solution were prepared as scavenging agents. To ensure that each bumblebee has equal access to the food and minimize inter-cage variability, 20 bumblebees in each group housed in four microcolony-rearing cages (5 bumblebees per cage) were treated with the contaminated pollen balls and the microparticles-based scavenging agents simultaneously. Pollen balls were prepared by mixing various insecticides with 10 g of high-desert bee pollen granules, followed by shaking until a homogeneous slurry was formed and full absorption of insecticides was achieved. The insecticide-containing pollen was rolled with sucrose into pollen balls by hand to obtain contaminated pollen balls. Microparticles dispersed in a sucrose solution (2 g ml^{-1}) were prepared as scavenging agents. Bumblebees (20 per group) placed in microcolony-rearing cages were treated with the contaminated pollen balls and the microparticle-based scavenging agents simultaneously. Microcolonies were observed every 12 h for mortality monitor until all bees deceased or 10 days had elapsed. On day 10, the heads of bumblebees detoxified by MTSMs were harvested, ground and homogenized to extract the bumblebee cells. The changes in AChE activity were then detected using the same method as described above.

Environmental safety

The safety profile of MTSMs was further investigated in insect models (*T. mitratus* and *T. emma*) and leguminous crops (soybean, *G. max* and mung bean, *V. radiata*). The *T. mitratus* and *T. emma* used for environmental safety evaluation were purchased from Qingdao Darunfucheng Animal Husbandry. The insects were maintained in ventilated containers (100 cm × 90 cm × 30 cm), each housing 20 individuals. The breeding environment was maintained at 22–30 °C with 40–60% relative humidity and a daily lighting period of over 6 h. A 3- to 5-cm layer of moist kitchen paper simulated natural substrate conditions for burrowing behaviour. Nutritional requirements were met through a combination diet of high-fibre oatmeal and commercial fish feed. For insect trials, *T. mitratus* or *T. emma* (n = 20 per group) were randomly allocated into experimental and control groups and housed in species-appropriate rearing cages. The treatment group received ad libitum access to standard feed pellets containing MTSMs (10 mg g^{-1}), while controls were provided unmodified feed. Mortality was assessed using standardized vitality criteria within 10 days. Concurrently, legume germination studies used the supernatant of MTSM suspension (20 mg ml^{-1}) for mung beans and soybeans in the treatment group, while the control group received tap water for germination and growth (n = 20 per group). Under optimal growth conditions (25 °C, 8/16 h light/dark), the germination rate, and root and shoot growth lengths were recorded. All experiments included triplicate trials with randomized block designs to ensure statistical validity.

We comprehensively assessed the ecological effects of MTSMs through analysis of postdigestive residues in bumblebee faeces. Bumblebees were first fed with MTSM-fortified sucrose solution to collect faeces for subsequent evaluation. *T. mitratus* or *T. emma* (n = 20 per group) were randomly allocated and housed in species-appropriate rearing cages. The treatment group received feed pellets supplemented with MTSM-containing faecal matrix (10 mg g^{-1}), while the control group was maintained on standard feed. Mortality was monitored every 12 h. To assess phytotoxic effects, the germination and growth of mung beans and soybeans in precisely regulated growth chambers (25 °C, 16/8 h light/dark cycle) were monitored. Experimental groups received the supernatant of MTSM suspension (20 mg ml^{-1}), while the control group was given tap water. Germination rates and growth lengths were quantitatively measured daily.

Statistical analysis

Data were represented as mean ± s.d. All statistical analyses were performed using GraphPad Prism software (v. 8.0.2, GraphPad Software). For comparison between the two groups, *P*-values were derived from an unpaired Student's *t*-test. For multiple group comparisons, one-way analysis of variance (ANOVA) with Tukey's multiple-comparisons test was empolyed. For survival analysis, the log-rank (Mantel–Cox) test was applied. Statistical significance was defined as $^{*}P < 0.05$, $^{**}P < 0.01$, $^{***}P < 0.001$, $^{****}P < 0.0001$; NS indicates no significance.

Reporting summary

Further information on the research design is available in the Nature Research Reporting Summary linked to this article.

Data availability

The authors declare that the data supporting the findings of this study are available within the paper and its Supplementary Information. Source data are provided with this paper.

References

1. Lemanski, N. J., Williams, N. M. & Winfree, R. Greater bee diversity is needed to maintain crop pollination over time. *Nat. Ecol. Evol.* **6**, 1516–1523 (2022).
2. Bascompte, J. & Scheffer, M. The resilience of plant–pollinator networks. *Annu. Rev. Entomol.* **68**, 363–380 (2023).
3. Garibaldi, L. A., Requier, F., Rollin, O. & Andersson, G. K. S. Towards an integrated species and habitat management of crop pollination. *Curr. Opin. Insect Sci.* **21**, 105–114 (2017).
4. Goulson, D., Nicholls, E., Botías, C. & Rotheray, E. L. Bee declines driven by combined stress from parasites, pesticides, and lack of flowers. *Science* **347**, 1255957 (2015).
5. Varah, A. et al. The costs of human-induced evolution in an agricultural system. *Nat. Sustain.* **3**, 63–71 (2020).
6. Fu, H. Y. et al. Advances in organophosphorus pesticides pollution: current status and challenges in ecotoxicological, sustainable agriculture, and degradation strategies. *J. Hazard. Mater.* **424**, 127–147 (2022).
7. Osaka, A. et al. Exposure characterization of three major insecticide lines in urine of young children in Japan—neonicotinoids, organophosphates, and pyrethroids. *Environ. Res.* **147**, 89–96 (2016).
8. Zhang, X. D. et al. Environmental occurrence, toxicity concerns, and biodegradation of neonicotinoid insecticides. *Environ. Res.* **218**, 15 (2023).
9. Ni, J. B. et al. Efficient degradation of imidacloprid by surface discharge cold plasma: mechanism of interaction between ROS and molecular structure and evaluation of residual toxicity. *J. Hazard. Mater.* **465**, 133066 (2024).
10. Park, H. et al. Magnetite nanoparticles as efficient materials for removal of glyphosate from water. *Nat. Sustain.* **3**, 129–135 (2020).
11. Chen, Y. J. et al. Cell-membrane-cloaked oil nanosponges enable dual-modal detoxification. *ACS Nano* **13**, 7209–7215 (2019).
12. Zou, S. J. et al. Dual-modal nanoscavenger for detoxification of organophosphorus compounds. *ACS Appl. Mater. Interfaces* **14**, 42454–42467 (2022).
13. Chen, J. et al. Pollen-inspired enzymatic microparticles to reduce organophosphate toxicity in managed pollinators. *Nat. Food* **2**, 339–347 (2021).
14. Vallet-Regí, M., Schüth, F., Lozano, D., Colilla, M. & Manzano, M. Engineering mesoporous silica nanoparticles for drug delivery: where are we after two decades? *Chem. Soc. Rev.* **51**, 5365–5451 (2022).
15. Feng, Y. et al. Mesoporous silica nanoparticles-based nanoplatforms: basic construction, current state, and emerging applications in anticancer therapeutics. *Adv. Healthc. Mater.* **12**, e2201884 (2023).

16. Li, X. D. et al. ROS-responsive Janus Au/mesoporous silica core/shell nanoparticles for drug delivery and long-term CT imaging tracking of MSCs in pulmonary fibrosis treatment. *ACS Nano* **17**, 6387–6399 (2023).
17. Cui, C. Y. & Liu, W. G. Recent advances in wet adhesives: adhesion mechanism, design principle and applications. *Prog. Polym. Sci.* **116**, 34 (2021).
18. Yang, Y. et al. Ultra-durable cell-free bioactive hydrogel with fast shape memory and on-demand drug release for cartilage regeneration. *Nat. Commun.* **14**, 7771 (2023).
19. Li, Z. et al. A multifunctional nanoparticle mitigating cytokine storm by scavenging multiple inflammatory mediators of sepsis. *ACS Nano* **17**, 8551–8563 (2023).
20. Zhang, Y. et al. Functional and binding studies of gallic acid showing platelet aggregation inhibitory effect as a thrombin inhibitor. *Chin. Herb. Med.* **14**, 303–309 (2022).
21. O'Reilly, A. D. & Stanley, D. A. Solitary bee behaviour and pollination service delivery is differentially impacted by neonicotinoid and pyrethroid insecticides. *Sci. Total Environ.* **894**, 164399 (2023).
22. Fu, M. et al. Cancer treatment: from traditional Chinese herbal medicine to the liposome delivery system. *Acta Mater. Med.* **1**, 486–506 (2022).
23. Čadež, T., Kolić, D., Šinko, G. & Kovarik, Z. Assessment of four organophosphorus pesticides as inhibitors of human acetylcholinesterase and butyrylcholinesterase. *Sci. Rep.* **11**, 21486 (2021).
24. Yang, L. M., Qu, L. J., Zhang, X. L., Li, M. M. & Liu, Z. Aptamer-induced in-situ growth of acetylcholinesterase–$Cu_3(PO_4)_2$ hybrid nanoflowers for electrochemical detection of organophosphorus inhibitors. *Nano Res.* **16**, 12134–12143 (2023).
25. Perry, T. et al. Role of nicotinic acetylcholine receptor subunits in the mode of action of neonicotinoid, sulfoximine and spinosyn insecticides in *Drosophila melanogaster*. *Insect Biochem. Mol. Biol.* **131**, 103547 (2021).
26. Thany, S. H. Molecular mechanism of action of neonicotinoid insecticides. *Int. J. Mol. Sci.* **24**, 4 (2023).
27. Lu, K. et al. Characterization of heat shock protein 70 transcript from *Nilaparvata lugens* (Stal): its response to temperature and insecticide stresses. *Pest. Biochem. Physiol.* **142**, 102–110 (2017).
28. Li, J. J. et al. Depolymerization and characterization of *Acacia mangium* tannin for the preparation of mussel-inspired fast-curing tannin-based phenolic resins. *Chem. Eng. J.* **370**, 420–431 (2019).
29. Zhang, J. et al. RNA interference revealed the roles of two carboxylesterase genes in insecticide detoxification in *Locusta migratoria*. *Chemosphere* **93**, 1207–1215 (2013).
30. Huang, Z. et al. Insect transient receptor potential vanilloid channels as potential targets of insecticides. *Dev. Comp. Immunol.* **148**, 104899 (2023).
31. An, Y. Q. et al. Engineered cell membrane coating technologies for biomedical applications: from nanoscale to macroscale. *ACS Nano* **19**, 11517–11546 (2025).
32. Ellman, G. L., Courtney, K. D., Andres, V. & Featherstone, R. M. A new and rapid colorimetric determination of acetylcholinesterase activity. *Biochem. Pharmacol.* **7**, 88–90 (1961).
33. Vlogiannitis, S. et al. Reduced proinsecticide activation by cytochrome P450 confers coumaphos resistance in the major bee parasite *Varroa destructor*. *Proc. Natl. Acad. Sci. USA* **118**, 7 (2021).
34. Chen, Q. et al. MOF-derived Co_3O_4@Co–Fe oxide double-shelled nanocages as multi-functional specific peroxidase-like nanozyme catalysts for chemo/biosensing and dye degradation. *Chem. Eng. J.* **395**, 125130 (2020).
35. Simo, C. et al. Urease-powered nanobots for radionuclide bladder cancer therapy. *Nat. Nanotechnol.* **19**, 554–564 (2024).
36. Cappa, F., Baracchi, D. & Cervo, R. Biopesticides and insect pollinators: detrimental effects, outdated guidelines, and future directions. *Sci. Total Environ.* **837**, 155714 (2022).
37. Ma, X. J. et al. Multifunctional Fe-doped carbon dots and metal-organic frameworks nanoreactor for cascade degradation and detection of organophosphorus pesticides. *Chem. Eng. J.* **464**, 10 (2023).
38. Shi, Y. et al. *π–π* stacking increases the stability and loading capacity of thermosensitive polymeric micelles for chemotherapeutic drugs. *Biomacromolecules* **14**, 1826–1837 (2013).
39. Gu, X. et al. cRGD-decorated biodegradable polytyrosine nanoparticles for robust encapsulation and targeted delivery of doxorubicin to colorectal cancer in vivo. *J. Control. Release* **301**, 110–118 (2019).
40. Xie, J. G. et al. Codelivery of BCL2 and MCL1 inhibitors enabled by phenylboronic acid-functionalized polypeptide nanovehicles for synergetic and potent therapy of acute myeloid leukemia. *Adv. Sci.* **10**, e2204866 (2023).
41. Song, Y. et al. An integrated quorum quenching biocatalytic nanoplatform for synergistic chemo-photothermal eradication of *P. aeruginosa* biofilm infections. *Acta Biomater.* **171**, 532–542 (2023).
42. Yang, Y. Y. et al. Global honeybee health decline factors and potential conservation techniques. *Food Secur.* **15**, 855–875 (2023).
43. Ma, W. H. Comparative study on the activity of digestive enzymes in salivary gland and midgut of Italian honeybee workers. *Agric. Handb.* **30**, 724–727 (2011).
44. Aylanc, V., Falcão, S. I. & Vilas-Boas, M. Bee pollen and bee bread nutritional potential: chemical composition and macronutrient digestibility under in vitro gastrointestinal system. *Food Chem.* **413**, 135597 (2023).
45. Brys, M. S., Skowronek, P. & Strachecka, A. Pollen diet—properties and impact on a bee colony. *Insects* **12**, 9 (2021).
46. Chen, Y. R., Tzeng, D. T. W. & Yang, E. C. Chronic effects of imidacloprid on honey bee worker development molecular pathway perspectives. *Int. J. Mol. Sci.* **22**, 23 (2021).
47. Cresswell, J. E., Robert, F. X. L., Florance, H. & Smirnoff, N. Clearance of ingested neonicotinoid pesticide (imidacloprid) in honey bees (*Apis mellifera*) and bumblebees (*Bombus terrestris*). *Pest. Manag. Sci.* **70**, 332–337 (2014).
48. Menzel, R. & Muller, U. Learning and memory in honeybees: from behavior to neural substrates. *Annu. Rev. Neurosci.* **19**, 379–404 (1996).
49. Mu, X. H. et al. Single-nucleus and spatial transcriptomics identify brain landscape of gene regulatory networks associated with behavioral maturation in honeybees. *Nat. Commun.* **16**, 3343 (2025).
50. Caserto, J. S. et al. Ingestible hydrogel microparticles improve bee health after pesticide exposure. *Nat. Sustain.* **7**, 1441–1451 (2024).
51. Ganie, S. Y., Javaid, D., Hajam, Y. A. & Reshi, M. S. Mechanisms and treatment strategies of organophosphate pesticide induced neurotoxicity in humans: a critical appraisal. *Toxicology* **472**, 153181 (2022).
52. Pulkrabkova, L. et al. Neurotoxicity evoked by organophosphates and available countermeasures. *Arch. Toxicol.* **97**, 39–72 (2023).
53. Wang, Y. X. et al. Enantioselective oral absorption of molecular chiral mesoporous silica nanoparticles. *Adv. Mater.* **35**, 2307900 (2023).
54. Yim, W. et al. Polyphenol-stabilized coacervates for enzyme-triggered drug delivery. *Nat. Commun.* **15**, 7295 (2024).
55. Cruz, V. A., Vicentini-Polette, C. M., Magalhaes, D. R. & de Oliveira, A. L. Extraction, characterization, and use of edible insect oil—a review. *Food Chem.* **463**, 141199 (2025).
56. Croissant, J. G., Butler, K. S., Zink, J. I. & Brinker, C. J. Synthetic amorphous silica nanoparticles: toxicity, biomedical and environmental implications. *Nat. Rev. Mater.* **5**, 886–909 (2020).

57. Arrese, E. L. & Soulages, J. L. Insect fat body: energy, metabolism, and regulation. *Annu. Rev. Entomol.* **55**, 207–225 (2010).
58. Zhang, Q. Z. et al. Neutrophil membrane-coated nanoparticles inhibit synovial inflammation and alleviate joint damage in inflammatory arthritis. *Nat. Nanotechnol.* **13**, 1182–1190 (2018).
59. Liu, L. Z. et al. Systematic design of cell membrane coating to improve tumor targeting of nanoparticles. *Nat. Commun.* **13**, 6181 (2022).
60. Ma, J. N. et al. Tumor microenvironment targeting system for glioma treatment via fusion cell membrane coating nanotechnology. *Biomaterials* **295**, 122026 (2023).

Author contributions

Z.H. and Y.W. contributed equally to this work as co-first authors. Z.H. and Y.W. conceived the study and designed the experiments. Z.H., Y.W., J. Guo, S.L. and J. Gui carried out experiments and collected data. Z.H. performed statistical analysis and data interpretation. Z.H. wrote the original draft. C.D., J.C. and Z.Z. conceived the study, supervised the work, acquired funding and revised the paper (co-corresponding authors). All authors read and approved the final paper.

Funding

This work was supported by grants from the National Key R&D Program of China (numbers 2024YFA1209900, 2024YFA1209901, 2022YFB3804600), the National Natural Science Foundation of China (numbers 82305052, 52373299), the Young Elite Scientists Sponsorship Program by CAST (2022-QNRC1-04) and the Jiangsu Specially-Appointed Professors Program (number 013074004038).

Competing interests

The authors declare no competing interest.

Additional information

Supplementary information The online version contains supplementary material available at https://doi.org/10.1038/s41893-026-01867-y.

Correspondence and requests for materials should be addressed to Zhiyuan Zhong, Jing Chen or Chao Deng.

Peer review information *Nature Sustainability* thanks Vesa-Pekka Lehto, Dengjun Wang, Ge Zhang and the other, anonymous, reviewer(s) for their contribution to the peer review of this work.

nature portfolio

Corresponding author(s): Chao Deng

Last updated by author(s): Apr 10, 2026

Reporting Summary

Nature Portfolio wishes to improve the reproducibility of the work that we publish. This form provides structure for consistency and transparency in reporting. For further information on Nature Portfolio policies, see our Editorial Policies and the Editorial Policy Checklist.

Statistics

For all statistical analyses, confirm that the following items are present in the figure legend, table legend, main text, or Methods section.

n/a	Confirmed
☐	☒ The exact sample size (*n*) for each experimental group/condition, given as a discrete number and unit of measurement
☐	☒ A statement on whether measurements were taken from distinct samples or whether the same sample was measured repeatedly
☐	☒ The statistical test(s) used AND whether they are one- or two-sided *Only common tests should be described solely by name; describe more complex techniques in the Methods section.*
☒	☐ A description of all covariates tested
☒	☐ A description of any assumptions or corrections, such as tests of normality and adjustment for multiple comparisons
☐	☒ A full description of the statistical parameters including central tendency (e.g. means) or other basic estimates (e.g. regression coefficient) AND variation (e.g. standard deviation) or associated estimates of uncertainty (e.g. confidence intervals)
☐	☒ For null hypothesis testing, the test statistic (e.g. *F*, *t*, *r*) with confidence intervals, effect sizes, degrees of freedom and *P* value noted *Give P values as exact values whenever suitable.*
☒	☐ For Bayesian analysis, information on the choice of priors and Markov chain Monte Carlo settings
☒	☐ For hierarchical and complex designs, identification of the appropriate level for tests and full reporting of outcomes
☒	☐ Estimates of effect sizes (e.g. Cohen's *d*, Pearson's *r*), indicating how they were calculated

Our web collection on statistics for biologists contains articles on many of the points above.

Software and code

Policy information about availability of computer code

Data collection	Microparticles morphology were observed with a Hitachi SU8010 scanning electron microscope. Surface area and pore size distribution was determined with an ASAP 2460 micromeritics. Microparticles were analyzed with a Tensor 27 fourier infrared spectromeritic and a SDT Q600 thermogravimeter. All CLSM images was obtained with a Zeiss 710 confocal micriscope. All UVabsorptions were obtained with a Varioskan LUX multifunctional enzyme marker and a Waters Alliance HPLC
Data analysis	All statistical analyses were performed on Graphpad Prism(version 8.0.2). All the microparticles imager were analyzed with ImageJ software (64-bit Java 1.8.0_172).

For manuscripts utilizing custom algorithms or software that are central to the research but not yet described in published literature, software must be made available to editors and reviewers. We strongly encourage code deposition in a community repository (e.g. GitHub). See the Nature Portfolio guidelines for submitting code & software for further information.

Data

Policy information about availability of data

All manuscripts must include a data availability statement. This statement should provide the following information, where applicable:

- Accession codes, unique identifiers, or web links for publicly available datasets
- A description of any restrictions on data availability
- For clinical datasets or third party data, please ensure that the statement adheres to our policy

Provide your data availability statement here.

Research involving human participants, their data, or biological material

Policy information about studies with human participants or human data. See also policy information about sex, gender (identity/presentation), and sexual orientation and race, ethnicity and racism.

Reporting on sex and gender	*Use the terms sex (biological attribute) and gender (shaped by social and cultural circumstances) carefully in order to avoid confusing both terms. Indicate if findings apply to only one sex or gender; describe whether sex and gender were considered in study design; whether sex and/or gender was determined based on self-reporting or assigned and methods used.* *Provide in the source data disaggregated sex and gender data, where this information has been collected, and if consent has been obtained for sharing of individual-level data; provide overall numbers in this Reporting Summary. Please state if this information has not been collected.* *Report sex- and gender-based analyses where performed, justify reasons for lack of sex- and gender-based analysis.*
Reporting on race, ethnicity, or other socially relevant groupings	*Please specify the socially constructed or socially relevant categorization variable(s) used in your manuscript and explain why they were used. Please note that such variables should not be used as proxies for other socially constructed/relevant variables (for example, race or ethnicity should not be used as a proxy for socioeconomic status).* *Provide clear definitions of the relevant terms used, how they were provided (by the participants/respondents, the researchers, or third parties), and the method(s) used to classify people into the different categories (e.g. self-report, census or administrative data, social media data, etc.)* *Please provide details about how you controlled for confounding variables in your analyses.*
Population characteristics	*Describe the covariate-relevant population characteristics of the human research participants (e.g. age, genotypic information, past and current diagnosis and treatment categories). If you filled out the behavioural & social sciences study design questions and have nothing to add here, write "See above."*
Recruitment	*Describe how participants were recruited. Outline any potential self-selection bias or other biases that may be present and how these are likely to impact results.*
Ethics oversight	*Identify the organization(s) that approved the study protocol.*

Note that full information on the approval of the study protocol must also be provided in the manuscript.

Field-specific reporting

Please select the one below that is the best fit for your research. If you are not sure, read the appropriate sections before making your selection.

☒ Life sciences ☐ Behavioural & social sciences ☐ Ecological, evolutionary & environmental sciences

For a reference copy of the document with all sections, see nature.com/documents/nr-reporting-summary-flat.pdf

Life sciences study design

All studies must disclose on these points even when the disclosure is negative.

Sample size	For the in vitro and in vivo experiments, we followed the standards for good scientific practice. We used at least 3 biological replicates per group, to calculate means and standard deviations and to perform statistical analyses.
Data exclusions	No data were excluded
Replication	Each experiment was replicated multiple times, and the replication numbers are listed both in 'Methodology' and below each figure. Replicates were reproducible
Randomization	All samples and organisms were randomly allocated into experimental groups.
Blinding	No formal blinding was used. The survival study was conducted by an independent operator, who was unaware of the treatment aonditions.

Reporting for specific materials, systems and methods

We require information from authors about some types of materials, experimental systems and methods used in many studies. Here, indicate whether each material, system or method listed is relevant to your study. If you are not sure if a list item applies to your research, read the appropriate section before selecting a response.

Materials & experimental systems

n/a	Involved in the study
☒	☐ Antibodies
☐	☒ Eukaryotic cell lines
☒	☐ Palaeontology and archaeology
☐	☒ Animals and other organisms
☒	☐ Clinical data
☒	☐ Dual use research of concern
☐	☒ Plants

Methods

n/a	Involved in the study
☒	☐ ChIP-seq
☒	☐ Flow cytometry
☒	☐ MRI-based neuroimaging

Eukaryotic cell lines

Policy information about cell lines and Sex and Gender in Research

Cell line source(s)	Locusta migratoria L. cell membrane
Authentication	Locusta migratoria L. were acquired from colonies of Soochow University
Mycoplasma contamination	No mycoplasma contamination was found
Commonly misidentified lines (See ICLAC register)	*Name any commonly misidentified cell lines used in the study and provide a rationale for their use.*

Animals and other research organisms

Policy information about studies involving animals; ARRIVE guidelines recommended for reporting animal research, and Sex and Gender in Research

Laboratory animals	B. impatiens (bumble bees) were acquired from Biobest. The Telepgryllus mitratus and emmas were acquired from Qindao Darunfucheng Animal Husbandry Co., Ltd.
Wild animals	The study did not involve wild animals
Reporting on sex	The study did not involve wild animals
Field-collected samples	The study did not involve samples collected from the field
Ethics oversight	The insects and young buds of lower plants involved in this research do not raise any ethical issues

Note that full information on the approval of the study protocol must also be provided in the manuscript.

Dual use research of concern

Policy information about dual use research of concern

Hazards

Could the accidental, deliberate or reckless misuse of agents or technologies generated in the work, or the application of information presented in the manuscript, pose a threat to:

No	Yes	
☐	☐	Public health
☐	☐	National security
☐	☐	Crops and/or livestock
☐	☐	Ecosystems
☐	☐	Any other significant area

Experiments of concern

Does the work involve any of these experiments of concern:

No	Yes	
☐	☐	Demonstrate how to render a vaccine ineffective
☐	☐	Confer resistance to therapeutically useful antibiotics or antiviral agents
☐	☐	Enhance the virulence of a pathogen or render a nonpathogen virulent
☐	☐	Increase transmissibility of a pathogen
☐	☐	Alter the host range of a pathogen
☐	☐	Enable evasion of diagnostic/detection modalities
☐	☐	Enable the weaponization of a biological agent or toxin
☐	☐	Any other potentially harmful combination of experiments and agents

Plants

Seed stocks

Report on the source of all seed stocks or other plant material used. If applicable, state the seed stock centre and catalogue number. If plant specimens were collected from the field, describe the collection location, date and sampling procedures.

Novel plant genotypes

Describe the methods by which all novel plant genotypes were produced. This includes those generated by transgenic approaches, gene editing, chemical/radiation-based mutagenesis and hybridization. For transgenic lines, describe the transformation method, the number of independent lines analyzed and the generation upon which experiments were performed. For gene-edited lines, describe the editor used, the endogenous sequence targeted for editing, the targeting guide RNA sequence (if applicable) and how the editor was applied.

Authentication

Describe any authentication procedures for each seed stock used or novel genotype generated. Describe any experiments used to assess the effect of a mutation and, where applicable, how potential secondary effects (e.g. second site T-DNA insertions, mosiacism, off-target gene editing) were examined.